Environment International 198 (2025) 109379

Contents lists available at ScienceDirect

Environment International

journal homepage: www.elsevier.com/locate/envint

Full length article

# Quanta emission rate during speaking and coughing mediated by indoor temperature and humidity

Vitor Lavor [a], Jianjian Wei [b], Omduth Coceal [c], Sue Grimmond [c], Zhiwen Luo [d,*]

[a] School of the Built Environment, University of Reading, Reading, UK
[b] Institute of Refrigeration and Cryogenics, Key Laboratory of Refrigeration and Cryogenics Technology of Zhejiang Province, Zhejiang University, Hangzhou, China
[c] Department of Meteorology, University of Reading, Reading, UK
[d] Welsh School of Architecture, Cardiff University, Cardiff, UK

ARTICLE INFO

*Keywords:*
Expiratory droplets
Quanta emission rate
Quanta
Indoor
Long-range airborne transmission

ABSTRACT

In epidemiological prospective modelling, assessing the hypothetical infectious quanta emission rate ($E_q$) is critical for estimating airborne infection risk. Existing $E_q$ models overlook environmental factors such as indoor relative humidity (RH) and temperature (T), despite their importance to droplet evaporation dynamics. Here we include these environmental factors in a prospective $E_q$ model based on the airborne probability functions with emitted droplet distribution for speaking and coughing activities. Our results show relative humidity and temperature have substantial influence on $E_q$. Drier environments exhibit a notable increase in suspended droplets (cf. moist environments), with $E_q$ having a 10-fold increase when RH decreases from 90 % to 20 % for coughing and a 2-fold increase for speaking at a representative summer indoor environment (T = 25° C). In warmer environments, $E_q$ values are consistently higher (cf. colder), with increases of up to 22 % for coughing and 9 % for speaking. This indicates temperature has a smaller impact than humidity. We demonstrate that indoor environmental conditions are important when quantifying the quanta emission rate using a prospective method. This is essential for assessing airborne infection risk.

## 1. Introduction

Transmission routes of respiratory pathogens are determined by how infectious respiratory particles (IRP) travel through the environment and how exposed people interact with them (Marr & Tang, 2021). The World Health Organization (WHO) suggests the terminologies of airborne (or inhalation), direct deposition and contact for the major modes of transmission of respiratory pathogens (Leung & Milton, 2024). The inhalation/airborne route occurs when expelled IRPs are inhaled and deposited in any site of the human respiratory tract, with can be subdivided into: (1) short-range: involving inhaling IRPs in close proximity (<1–2 m) (Li, 2021a), and (2) long-range: referring to inhalation of aerosols at greater distances (Duval et al., 2022).

Infection transmission risk can be estimated using Quantitative Microbial Risk Assessment (QMRA), with a dose–response model to predict the likelihood of infection based on exposure to a certain dose of pathogens (Sze To & Chao, 2010). The Wells-Riley equation, one of the most used QRMA methods for evaluating airborne infections, quantifies the risk probability by considering variables such as ventilation rate, exposure time and quanta emission rate ($E_q$) (Kurnitski et al., 2021). The Wells (1955) dimensionless quantum of contagion represents the infectious dose necessary to infect 63.2 % of susceptible individuals [i.e., (1 – 1/e)] with pathogens-to-quanta ratio varying by pathogen type (Mikszewski et al., 2022). The quantum accounts for both concentration and virulence of the infectious material in the air. The rate of infectious quanta that are released into the air from a person ($E_q$) is essential for modelling the spread of airborne diseases and implementing effective control methods (Jones et al., 2023).

Generally, two methods are used for estimating $E_q$. First, the retrospective method uses a past contamination airborne transmission outbreak event to estimate $E_q$ from epidemiological factors and ventilation rates (Miller et al., 2021). The outbreak data needed includes ventilation conditions (mechanical/natural ventilation), population density and behaviours, and ambient conditions. Insights derived from post-event data alone may be potentially delayed and could result in inaccurate estimates. Scarce data about variability of emission rates between emitters and through time may limit ability to extrapolate to other scenarios (Jones et al., 2024). Second, the prospective method (Buonanno, Stabile, and Morawska, 2020) estimates $E_q$ using the viral

* Corresponding author at: Welsh School of Architecture, Cardiff University, Cardiff, UK.
*E-mail address:* luoz18@cardiff.ac.uk (Z. Luo).

https://doi.org/10.1016/j.envint.2025.109379
Received 29 October 2024; Received in revised form 4 March 2025; Accepted 13 March 2025
Available online 14 March 2025

**Nomenclature**

| Variable | Meaning/Reference/Unit |
|---|---|
| $A_r$ | Attack rate Eq. (10) % |
| a, b, c | Fitted parameters in the sigmoid function Eq. (6) – |
| $c_i$ | Conversion factor Eq. (1) Quanta RNA copies$^{-1}$ |
| $C_n$ | Droplet number concentration Eq. (2), (4) Particles m$^{-3}$ |
| $c_v$ | Viral load Eq. (1) RNA copies mL$^{-1}$ |
| $D_{crit}$ | Maximum diameter of exhaled droplet Eq. (2) μm |
| $D_{i,med}$ | Count median diameter Eq. (4) μm |
| $D_{i,sd}$ | Geometric standard deviation Eq. (4) μm |
| $D_{p,0}$ | Initial diameter of droplets Eq. (2) μm |
| $E_q$ | Quanta emission rate Eq. (1), (10) Quanta h$^{-1}$ |
| $I$ | Number of infectors Eq. (10) person |
| $n$ | Number of samples Eq. (7)–(9)– |
| $N_{total}$ | Number of droplets released Eq. (5) – |
| $N_{ground}$ | Number of droplets settling to the ground Eq. (5) – |
| $p_r$ | Pulmonary ventilation rate Eq. (1), (10) m$^3$ h$^{-1}$ |
| $t_{ex}$ | Exposure time Eq. (10) h |
| T | Temperature Eq. (3) °C |
| $v$ | Volume concentration Eq. (1) mL m$^{-3}$ |
| $V$ | Volume of a single droplet Eq. (2) mL |
| $V_{venue}$ | Volume of the venue Eq. (10) m$^3$ |
| $x$ | Horizontal distance Eq. (5) m |
| $y_i$ | "True" value Eq. (7)–(9) – |
| $\hat{y}_i$ | Predicted value Eq. (7)–(9) – |
| $\bar{y}_i$ | Mean "true" value Eq. (7)–(9) – |
| $\lambda$ | Air changes per hour Eq. (10) h$^{-1}$ |
| $\gamma$ | Airborne probability Eq. (5) – |
| $\gamma_l$ | Long-range airborne probability Eq. (3), (6) – |
| MAE | Mean absolute error Eq. (7) – |
| MBE | Mean biased error Eq. (8) – |
| RH | Relative humidity Eq. (3) % |
| $R^2$ | Coefficient of determination Eq. (9) – |

load from IRPs and pathogen's infectivity data from measurements (e.g., aerosol samples and RT-qPCR (Stadnytskyi et al., 2020)), making it more reliable and applicable to various studies (Buonanno et al., 2022; Li et al., 2021; Mikszewski et al., 2022).

The prospective method quanta emission rate ($E_q$) [quanta h$^{-1}$] is estimated from (Buonanno, Stabile, and Morawska, 2020):

$$E_q = c_v c_i p_r v \tag{1}$$

where $c_v$ is the viral load of exhaled droplets [ribonucleic acid (RNA) copies mL$^{-1}$], $c_i$ is the conversion factor [quanta RNA copies$^{-1}$], and $p_r$ is the pulmonary ventilation rate of the infected person [m$^3$ h$^{-1}$]. The volume concentration of exhaled droplets [mL m$^{-3}$] $v$ is calculated by integrating over the volumes of droplets of initial diameter $D_{p,0}$:

$$v = \int_0^{D_{crit}} C_n(D_{p,0})\, dV(D_{p,0}) \tag{2}$$

where $C_n$ is the droplet number concentration [particles m$^{-3}$] and $V$ is the volume of a single droplet [mL]. The critical droplet diameter [μm] $D_{crit}$ is essential for understanding particle behaviour dynamics in respiratory emissions. For a given ambient condition, $D_{crit}$ indicates the threshold between droplets with $D_{p,0} > D_{crit}$ that settles due to gravity and droplets with $D_{p,0} < D_{crit}$ that evaporate fully before settling (Chaudhuri et al., 2020; Xie et al., 2007). $D_{crit}$ indicates the boundary between the inhalation/airborne to other transmission modes, since the former involves droplets that no longer remain suspended in the air.

Buonanno et al. (2020) originally used a $D_{crit}$ of 10 μm, while Li et al. (2021) used 20 μm suggesting only IRPs that shrink to around 5–10 μm in diameter should be accounted for in the inhalation transmission route. These $D_{crit}$ values were likely chosen for simplicity, assuming that inhalation transmission occurs only if IRPs are < 5 μm in diameter (Li et al., 2022). This is now considered outdated (Jimenez et al., 2022), as there is evidence that IRPs dynamics are environment-dependent, with settling rate and spread distance influenced by various factors including droplet size, internal content, exhalation mode, speed and direction, expired jet flow instabilities, ambient air temperature (T) and relative humidity (RH) (Cavazzuti & Tartarini, 2023; Chaudhuri et al., 2020; Liu et al., 2017; Wei & Li, 2015). For example, Xie et al. (2007) demonstrate $D_{crit}$ could vary from 95 to 65 μm (for RH of 30 % and 70 %) in an indoor environment with T = 20 °C, while Chaudhuri et al. (2020) found $D_{crit}$ can almost double when the indoor environment is warmed from 5 to 35 °C. Turbulence-induced exhaled jet fluctuations in droplet dispersion can cause up to a four-fold greater spread compared to cases where turbulence is disregarded (Wei & Li, 2015). Despite evidence of their importance, environmental characteristics are overlooked in estimating $E_q$ from both retrospective and prospective methods.

To better understand how indoor environmental factors influence the critical droplet diameter and hence $E_q$, we use a prospective approach and integrate the airborne probability of respirable-sized IRPs after modelling evaporation and transport for different indoor RH and T scenarios. The model results are used for deriving a simple parametrization for airborne probability in relation to environment conditions, to calculate $E_q$. We utilise our modified $E_q$ to simulate different outbreaks, which we compare to the previous Buonanno et al. (2020) case.

## 2. Methods

### 2.1. Modified quanta emission rate ($E_q$) estimation

Our modified prospective method is developed to improve understanding of how indoor environmental conditions affects $E_q$.

$$E_q = c_v c_i p_r \int_0^{D_{crit}=100\mu m} C_n(D_{p,0})\, \gamma_l(D_{p,0}, RH, T)\, dV(D_{p,0}) \tag{3}$$

where $\gamma_l$ is the airborne probability of droplets (Section 2.1.2). We consider both relative humidity (RH) in the range 20 to 100 % and indoor air temperature (T) of 18 and 25 °C to represent summer and winter indoor conditions of temperature-controlled environments (Salthammer & Morrison, 2022).

If IRPs settle on the ground, they no longer represent an inhalation transmission route risk. Hence, we include airborne probability (Wei & Li, 2015) to indicate the likelihood of IRPs remaining suspended in the air rather than settling at a specific distance (Grandoni et al., 2024; Wei & Li, 2015).

We set the upper limit of droplet size that can be inhaled by humans to 100 μm (Milton, 2020) as a more realistic cut-off for $D_{crit}$ for the inhalation route. Turbulence can enhance the dispersion and spread of expired IRPs and this is captured by the airborne probability, as large dried-out droplets (> 50 μm) can be found up to 4 m from the emitter when coughing is considered (Wei & Li, 2015). Even low probabilities of larger droplets reaching longer distances may have important implications for the airborne disease transmission.

#### 2.1.1. Droplet size distribution

We adopt Johnson et al. (2011)'s droplet number concentration ($C_n$) from their trimodal distribution (Table 1) for speaking and coughing activities. It allows IRPs to be released from different origins in the

**Table 1**
Trimodal droplet size distribution model parameters for coughing and speaking (Johnson et al., 2011) including diameter geometric standard deviation ($D_{i,sd}$) and count median diameter ($D_{i,med}$).

| | Coughing | | | Speaking | | |
|---|---|---|---|---|---|---|
| **Mode** | Bronchiolar | Laryngeal | Oral | Bronchiolar | Laryngeal | Oral |
| $C_n$ [cm$^{-3}$] | 0.0903 | 0.1419 | 0.0159 | 0.054 | 0.0684 | 0.00126 |
| $D_{i,med}$ [μm] | 2.4123 | 2.4615 | 123.3 | 2.4830 | 3.6923 | 144.6 |
| $D_{i,sd}$ [μm] | 1.25 | 1.68 | 1.837 | 1.30 | 1.66 | 1.795 |

respiratory tract, including bronchiolar, laryngeal, and oral sites.

$$\frac{dC_n}{dLogD_{p,0}} = \ln(10)x\sum_{i=1}^{3}\left(\frac{C_{n,i}}{\sqrt{2\pi}\ln(D_{i,sd})}\right)\exp\left(-\frac{(\ln D_{p,0}-\ln(D_{i,med}))^2}{2(\ln D_{i,sd})^2}\right) \quad (4)$$

### 2.1.2. Airborne probability ($\gamma$)

Droplets that settle on the ground are removed from the air, so no longer represent an inhalation transmission risk. By introducing the airborne probability of droplets ($\gamma$) we consider turbulence-induced exhaled jet fluctuations and their impact on dispersion using a discrete random walk approach. The $\gamma$ term gives the likelihood of IRPs remaining suspended in the air, by the quantity that settle to the ground, $N_{ground}(x)$, at a specific distance $x$ relative to the total number of droplets released, $N_{total}$ (Grandoni et al., 2024; Wei & Li, 2015):

$$\gamma = 1 - \frac{N_{ground}(x)}{N_{total}} \quad (5)$$

As we consider only IRPs inhaled at a long-range, we calculate the long-range airborne probability ($\gamma_l$) for speaking using $x = 2$ m. For coughing a larger threshold of $x = 4$ m is adopted, as the cough jet can remain suspended in the air for longer compared to speaking breaths (Bourouiba, 2020).

### 2.1.3. Droplet movement and evaporation

The long-range airborne probability ($\gamma_l$) requires information of movement and evaporation of exhaled IRPs to be modelled. The initial velocity of an exhaled droplet depends on respiratory activity. Once exhaled evaporation will cause the droplet to start to lose water to the ambient air. Key model assumptions are (details in Appendix and Wei & Li, 2015):

- Exhaled droplets are spherical during transport.
- Thermophysical properties are uniform within the droplet.
- Heat transfer processes through the droplet surface are convective heating and evaporative cooling.
- Exhaled droplets contain both soluble and insoluble components. Vapour pressure at the droplet surface depend on Kelvin and solute effects.
- Droplets are emitted together with breathing air in a turbulent buoyant round jet, with a discrete random walk representing in-jet turbulence.

## 2.2. Cases simulated

The two indoor air temperatures considered, warm (T = 25 °C) and cool (T = 18 °C), are intended to represent typical summer and winter indoor conditions in temperature-controlled environments in Europe (Salthammer & Morrison, 2022). Obviously, values vary associated with regional and cultural factors. Eight relative humidity conditions are selected to cover a range of indoor humidity scenarios. These span 20 to 90 %, at 10 % intervals. The exhaled droplets range in diameter from 10 to 100 μ m (interval = 2 μm), aligning with the upper limit of droplet diameter that can be inhaled by humans (Milton, 2020).

The epidemiological parameters are fixed for all simulations to estimate the quanta emission rate, using the volume concentration from Eq. (2). The median epidemiological parameter values for SARS-CoV-2 are used for viral load $c_v$ (= 4x10$^5$ RNA copies mL$^{-1}$) and conversion factor $c_i$ (= 0.0014 quanta RNA$^{-1}$) (Mikszewski et al., 2022). Pulmonary ventilation rate $p_r$ varies with respiratory activities, with speaking being 0.54 m$^3$ h$^{-1}$ (Mikszewski et al., 2022) and for coughing being 0.0144 m$^3$ h$^{-1}$ based on persistent coughing [frequency 9 coughs h$^{-1}$] with a coughing flow rate of 2.45 x10$^{-3}$ m$^3$ cough$^{-1}$ (Altshuler et al., 2023; Gupta et al., 2009). We use a constant coughing frequency of 9 per hour, whereas this can vary with contamination stage and pathogen (Altshuler et al., 2023).

Quanta emission rate is estimated based on the long-range airborne probability (Eq. (5) with 1000 exhaled droplets per simulation scenario. The exhalation velocity is kept constant at 5 (speaking) and 10 m s$^{-1}$ (coughing) with an exhaled air temperature set at 35 °C.

### 2.2.1. Parameterisation of long-range airborne probability ($\gamma_l$)

For computational efficiency a sigmoid equation is fit to the long-range airborne probability cases simulated:

$$\gamma_l = \frac{1}{1+\exp-(aD_{p,0}+bRH+c)} \quad (6)$$

where $a$, $b$ and $c$ are the fitted parameters. The sigmoid function provides a smooth, continuous approximation of the probability, capturing nonlinear relationships between the settling and evaporation processes. This allows a fast airborne probability estimate across the range of droplet sizes without needing detailed calculations, thus reducing computational resources needed.

With only two indoor temperature scenarios, parameters are derived for each reparatory activity and temperature condition (i.e., four sets of parameters or equations). The parameter fitting is done twice, with the results split by RH values into one (i.e., 20 – 90 %), and three (low: 20 – 40 %, medium: 50 – 60 % and high: 70 – 90 %) classes.

The fitted model accuracy is evaluated by assessing the predictive capacity for RH values used in the training (fitting) phase, using standard metrics:

(1) Mean absolute error (MAE):

$$\mathrm{MAE} = \frac{1}{n}\sum_{i=1}^{n}|y_i-\hat{y}_i| \quad (7)$$

(2) Mean biased error (MBE):

$$\mathrm{MBE} = \frac{1}{n}\sum_{i=1}^{n}(y_i-\hat{y}_i) \quad (8)$$

(3) Coefficient of determination (R$^2$):

$$\mathrm{R}^2 = \frac{\sum_{i=1}^{n}(y_i-\hat{y}_i)^2}{\sum_{i=1}^{n}(y_i-\bar{y})}$$

$$\bar{y}_i = \frac{1}{n}\sum_{i=1}^{n}y_i \quad (9)$$

where $\hat{y}_i$ is the predicted value of the $i$-th sample, with $y_i$ is the "true" value, and $\bar{y}$ is the mean of the true values.

### 2.3. Application to two outbreak case studies

We compare our results to retrospective assessments from two SARS-CoV-2 outbreak cases: an outbreak in a restaurant in Guangzhou, China (Lu et al., 2020) and in a call centre in South Korea (Prentiss et al., 2020). In the retrospective analysis, we estimate the quanta emission rate using the Wells-Riley equation, considering no other losses apart from ventilation at the time of the event:

$$A_r = 1 - \exp\left(\frac{I p_r E_q t_{ex}}{V_{venue}\lambda}\right) \quad (10)$$

where $A_r$ is the attack rate [%], $I$ is the number of infectors [person], $p_r$ is the pulmonary ventilation rate [$m^3\ h^{-1}$], $E_q$ is the quanta generation rate [quanta (h person)$^{-1}$], $t_{ex}$ is the exposure time interval [h], $V_{venue}$ is the volume of the venue [$m^3$] and $\lambda$ is the air changes per hour [$h^{-1}$].

Monte Carlo simulations (Kroese et al., 2014) are performed to estimate the $E_q$ for retrospective method for each outbreak location. Parameters from Eq. (10) are used in the range values and distribution specified in Table 2, where uncertainties are obtained by varying these parameters within their specified lower and upper limits (Lu et al., 2020; Prentiss et al., 2020).

Additionally, Monte Carlo simulations are also conducted for our proposed method using parameters from Eq. (1). The range of variables and their distributions, as shown in Table 3, are used to capture the uncertainties. This approach facilitates the analysis of the uncertainty estimates derived from both methods.

## 3. Results and Discussion

### 3.1. Droplet dispersion pattern

To determine the number of droplets needed to provide robust statistical results an initial sensitivity analysis (Fig. S.1) found 1,000 droplets to be enough. This involves releasing a single droplet every 0.04 s over a 40 s duration.

A snapshot of the droplet distribution in space at $t = 40$ s, with an initial size $D_{p,0}$ of 50 μm varies with humidity conditions (RH = 20 and 90 %) and between activities, speaking (Fig. 1a) and coughing (Fig. 1b), in the summer scenario (T = 25 °C). Medium-sized droplets predominantly follow the cough jet under dry environments for both coughing and speaking, as higher evaporation rate in lower RH conditions prolongs the presence of larger exhaled droplets in the environment. Wei & Li (2015) also highlighted the significant effect of evaporation on medium-sized droplets for coughing, while variations in RH have minimal impact on the airborne probability of small (< 30 μ m) and large droplets (> 60 μ m). Smaller droplets tend to follow the jet airflow closely, while larger droplets settle more quickly to the ground.

For both speaking and coughing, when the RH = 20 %, the airborne probability remains at 100 % across all considered distances (Fig. 1), indicating a tendency for dried-out droplets to follow jet streamlines in dry environments. In contrast, for wet environments with RH = 90 %, droplets are observed to settle at around 0.25 m from the emitter during speaking and 0.50 m during coughing with airborne probability decreasing to 0.15 and 0.25 for the largest distances considered, respectively, indicating reduced spread in more humid conditions.

**Table 2**
Parametric values used in the Monte Carlo simulation for estimating $E_q$ using the retrospective method in Equation (10) for a restaurant and a call centre (Lu et al., 2020; Prentiss et al., 2020).

| Parameter | Restaurant China | | Call Centre Korea | |
|---|---|---|---|---|
| | *Values* | *Distribution* | *Values* | *Distribution* |
| $A_r$ (%) | 0.45 – 0.81 | Uniform | 0.50 – 0.75 | Uniform |
| $p_r$ ($m^3\ h^{-1}$) | 0.49 – 1.38 | Uniform | 0.49 – 1.38 | Uniform |
| $\lambda$($h^{-1}$) | 0.56 – 0.77 | Uniform | 0.5 – 1.5 | Uniform |
| $V_{venue}$($m^3$) | 45 | Constant | 1143 | Constant |
| $t_{ex}$ (h) | 1 | Constant | 8 | Constant |

**Table 3**
Parametric values used in the Monte Carlo simulation for estimating our proposed method in Eq. (1) for simulated scenarios.

| Parameter | Summer | | Winter | |
|---|---|---|---|---|
| | *Values* | *Distribution* | *Values* | *Distribution* |
| $c_i$ (quanta RNA copies$^{-1}$) | 0.0014 | Constant | 0.0014 | Constant |
| $c_v$ (RNA copies mL$^{-1}$) | 5.6 (1.2) | $Log_{10}$ normal (mean/std dev) | 5.6 (1.2) | $Log_{10}$ normal (mean/std dev) |
| $p_r$ ($m^3\ h^{-1}$) | 0.49 – 1.38 | Uniform | 0.5 – 1.5 | Uniform |
| $v$ (mL $m^{-3}$) | 0.047 | Constant | 0.021 | Constant |
| RH (%) | 20 | Constant | 90 | Constant |

### 3.2. Long-range airborne probability of droplets

Long-range airborne probability of exhaled droplets ($\gamma_l$) is computed across various RH levels and droplet sizes for the winter and summer air temperatures. Threshold distances ($x_t$) are set to 2 m for speaking and 4 m for coughing, to allow the long-range inhalation route to be distinguished from the short-range (Eq. (5)).

There is a consistent decline in $\gamma_l$ with increasing droplet size and RH for both coughing and speaking activities (Fig. 2). Between $\gamma_l = 0.02$ (pink, Fig. 2) and green $\gamma_l = 0.98$ (green) is where most droplets are susceptible to fluctuation in long-range airborne probability. This indicates long-range airborne probability for medium-sized droplets (40 – 70 μm) are more influenced by external conditions, particularly in environments with low to medium RH (< 70 %). Although higher RH environments are expected to have fewer suspended droplets, a fraction of 50 $\mu$m droplets will persist (12.3 % for coughing and 6.6 % for speaking, with the winter T). Larger droplets are more susceptible to indoor temperature variations, as evidenced by the leftward shift of the $\gamma_l = 0.02$ bound from summer (pink solid, Fig. 2) to winter (dashed) for both respiratory activities. This shift indicates that droplets with same size evaporate more rapidly in higher temperature environments due to heightened vapour pressure deficit, resulting in a greater droplet suspension in the air.

The long-range airborne probability model parameters (Table 4) are derived from fitting Eq. (6) using One and Three RH classes approaches. The fits are verified using ambient RH of 35 % and 55 % (i.e., a low and medium case from the Three RH class approach), for data not used in the fitting stage.

Predictions for coughing activity (Fig. 3) have comparable performance between the One and Three class approach for RH = 35 % in both summer and winter temperatures. Both approaches show similar values for the metrics considered, despite the tendency to underestimate the actual values as indicated by negative MBE (Table 5). In contrast, for RH = 55 %, the Three class approach substantially outperforms the One class, exhibiting improved estimates based on MBE with smaller MAE and larger $R^2$ values (Table 5). Given the Three class approach's better predictability, particularly at higher RH, the long-range airborne probability is predicted using it when determining the quanta emission rate ($E_q$).

### 3.3. Quanta emission rate

Increasing temperature leads to an increase in $E_q$, while higher RH results in a decrease in $E_q$. Coughing indoors has a 10-fold larger $E_q$ if the RH is 20 % compared with 90 % (Fig. 4a), whilst for speaking the difference is only 2-fold for the same temperature conditions (Fig. 4b). As for the long-range airborne probability (Fig. 2), indoor temperature also influences the quanta emission rate across all RH levels (Fig. 4), with a more pronounced effect in drier environment. At T = 25 °C, the quanta

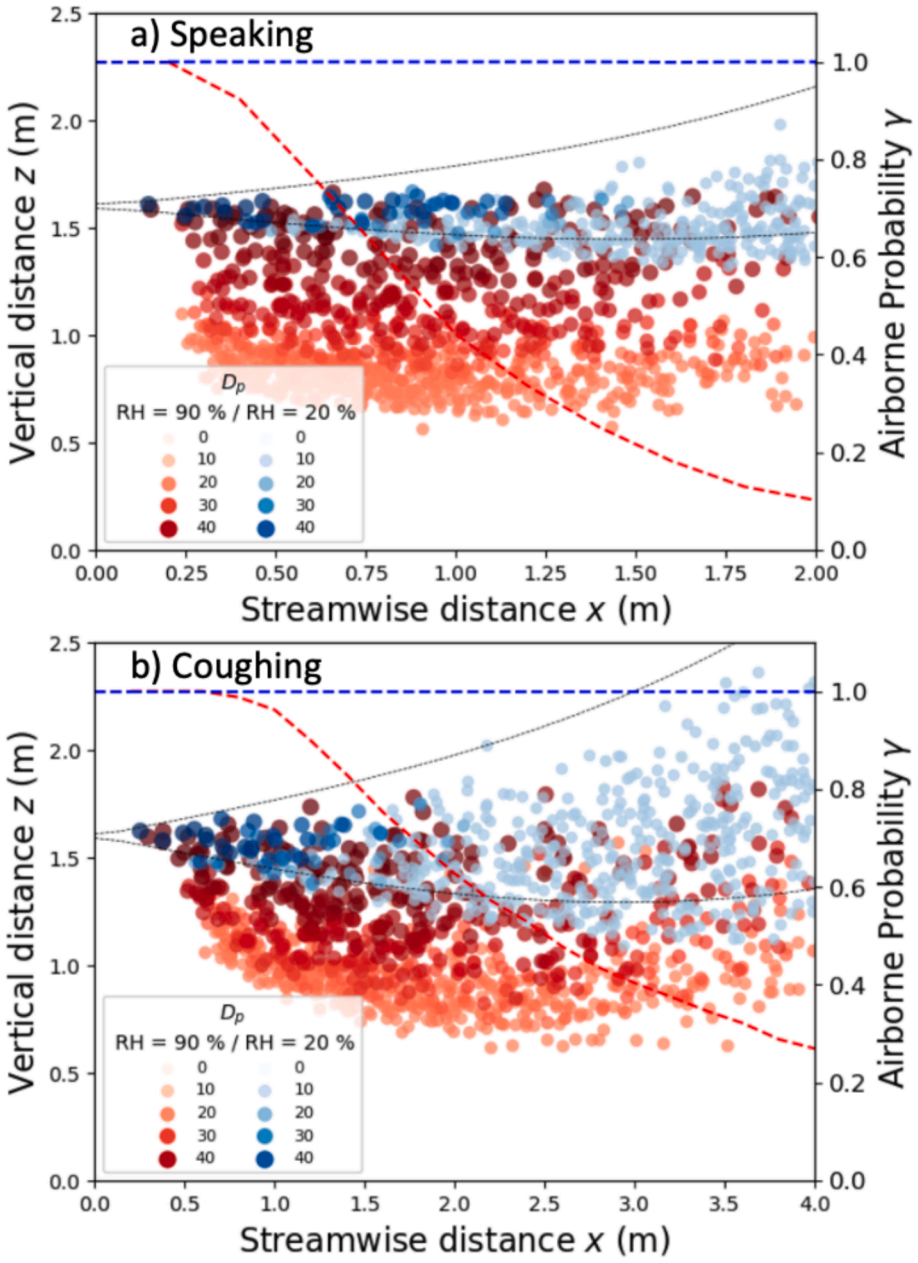


**Fig. 1.** Droplet distribution at t = 40 s for (**a**) speaking and (**b**) coughing for two ambient RH conditions (blue: 20 %, red: 90 %) with expiratory jet boundaries (black dashed lines) and airborne probability (blue, red, dashed lines, right-hand y-axis). The initial droplet diameter is 50 μm and T = 25 °C.

emission rate increases up to 19 % for coughing and 8 % for speaking (cf. T = 18 °C). By linearly extrapolating our data, environments with a lower temperature of T = 14 °C would experience a slight reduction in the quanta emission rate, with a 11 % decrease for coughing and 5 % decrease for speaking for drier environments, with smaller values observed at higher RH levels.

For speaking $E_q$ is larger than for coughing (Fig. 4), due to its higher frequency of occurrence. However, $E_q$ for coughing alone (assuming 9 coughs $h^{-1}$) constitute a substantial fraction of that for speaking, amounting to approximately 20 % in an environment with RH = 20 % and to 6 % in with RH = 90 %. Moreover, as a sick person may alternate between speaking and coughing, and also with higher frequency of coughing, this could potentially further increase $E_q$ values.

It is noteworthy that much lower estimates of $E_q$ are obtained using the original Buonanno et al. (2020) formulation with a $D_{crit}$ of 10 μm assumed. This large discrepancy arises from our approach accounting for the influence of larger droplets, which are more susceptible to environmental conditions. Hence, including this effect points to a greater potential for disease transmission.

### 3.4. Case study

In the following comparison, we explore the variability in calculated $E_q$ using Monte Carlo simulation (1000 runs) for a retrospective method for two outbreak scenarios and our proposed method (Section 2.3). Due to the absence of specific temperature and relative humidity (RH) values during the outbreaks (Lu et al., 2020; Prentiss et al., 2020) we applied our proposed method to two extreme scenarios in terms of $E_q$ estimates: dry and warm (RH = 20 % and T = 25 °C) and wet and cold (RH = 90 % and T = 18 °C). Additionally, we include the estimates using $D_{crit}$ = 10 μm (Buonanno et al., 2020) and present the results in interquartile ranges (IQR) to illustrate the variability of the estimates while minimizing the influence of extreme values (Fig. 5).

From the retrospective analysis, for a 1-hour event in a restaurant in

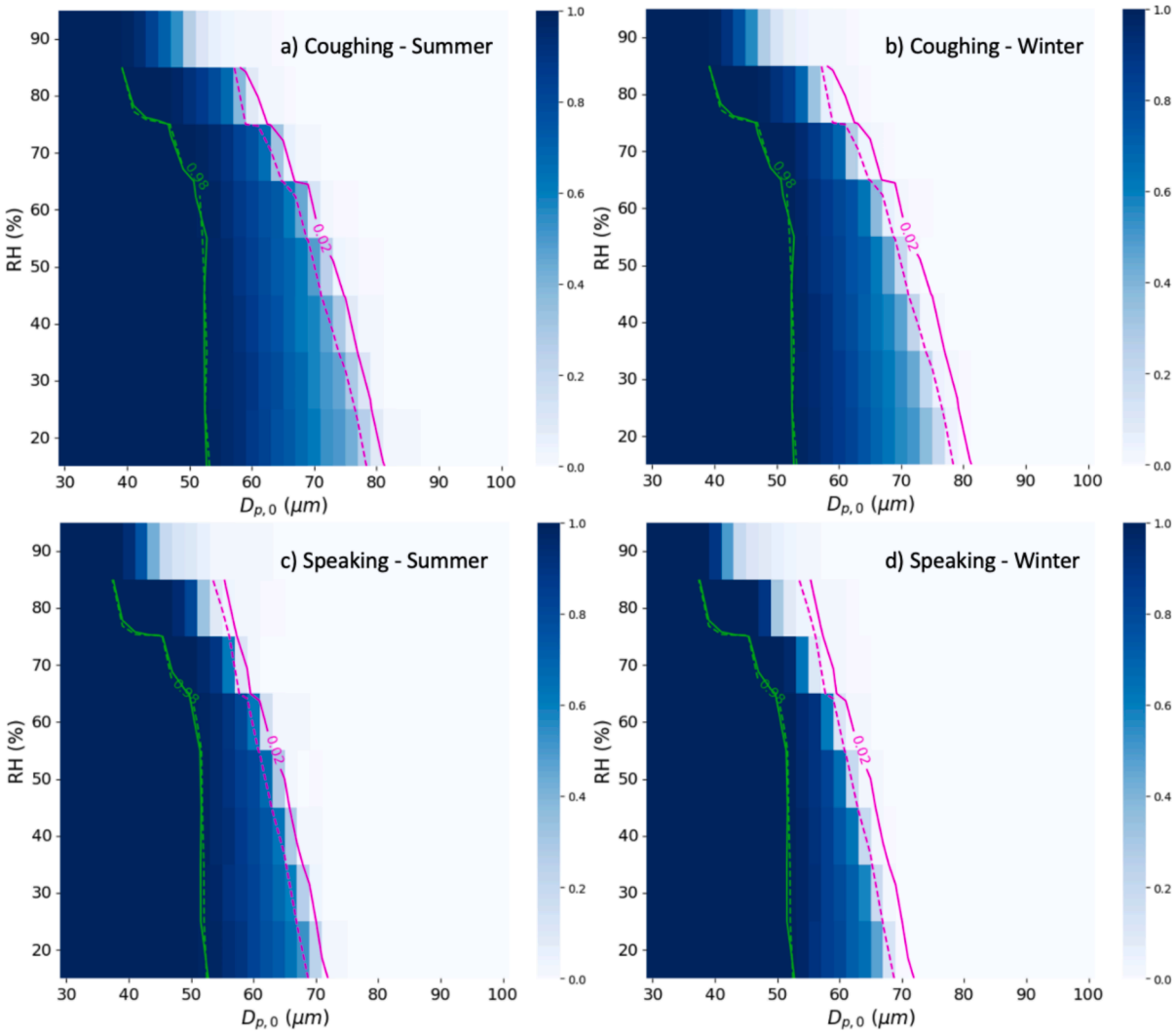


**Fig. 2.** Heat map of $\gamma_l$ in summer and winter for (a, b) coughing and (c, d) speaking with values $\gamma_l$ of 0.02 (pink) and 0.98 (green) when T = 25 °C (solid) and T = 18 °C (dashed).

**Table 4**
Fitted parameters for the sigmoid equation (Eq. (6)) using the One and Three RH classes approaches for summer and winter temperatures.

| Model | Summer (T = 25 °C) | | | Winter (T = 18 °C) | | |
|---|---|---|---|---|---|---|
| | a | b | c | a | b | c |
| Coughing One | −0.2659 | −0.0869 | 21.9210 | −0.3028 | −0.0974 | 24.3288 |
| Speaking One | −0.4307 | −0.1313 | 32.6496 | −0.4976 | −0.1470 | 36.5284 |
| Coughing Three - Low RH | -0.2207 | -0.0279 | 16.5011 | -0.2525 | -0.0319 | 18.4122 |
| Coughing Three - Medium RH | -0.3262 | -0.0707 | 25.8772 | -0.3958 | -0.0878 | 30.7511 |
| Coughing Three - High RH | -0.4852 | -0.3511 | 55.1593 | -0.5958 | -0.4233 | 66.0338 |
| Speaking Three - Low RH | -0.3990 | -0.0589 | 27.9199 | -0.4899 | -0.0683 | 33.1625 |
| Speaking Three - Medium RH | -0.6921 | -0.1629 | 51.4679 | -0.9694 | -0.2130 | 69.3234 |
| Speaking Three - High RH | -0.7873 | -0.4918 | 79.0972 | -1.0096 | -0.6153 | 98.4088 |

China the median value $E_q$ of 32.76 quanta $h^{-1}$ while it becomes 149.47 quanta $h^{-1}$ in an 8-hour shift in a call centre in South Korea (green, Fig. 5). Although retrospective and prospective methods are not directly comparable, estimating $E_q$ using our prospective model gives median $E_q$ of 2.78 to 5.93 quanta $h^{-1}$ for different environmental conditions, with lower values for when it is cold and wet (blue Fig. 5). Accounting for the environmental factors significantly influence quanta emission rates and provides a closer approximation to the retrospective data when compared to 0.21 quanta $h^{-1}$ obtained using the upper limit $D_{crit}$ = 10 μm as suggested by Buonanno et al. (2020) (yellow, Fig. 5).

By incorporating environmental variables, our model offers more accurate predictions of $E_q$. These results highlight the impact of seasonal and environmental factors. Recognizing these influences enables more robust risk assessments for airborne disease transmission and facilitates the development of targeted preventive measures, such as adjusting ventilation/heating strategies or implementing specific hygiene practices during high-risk periods.

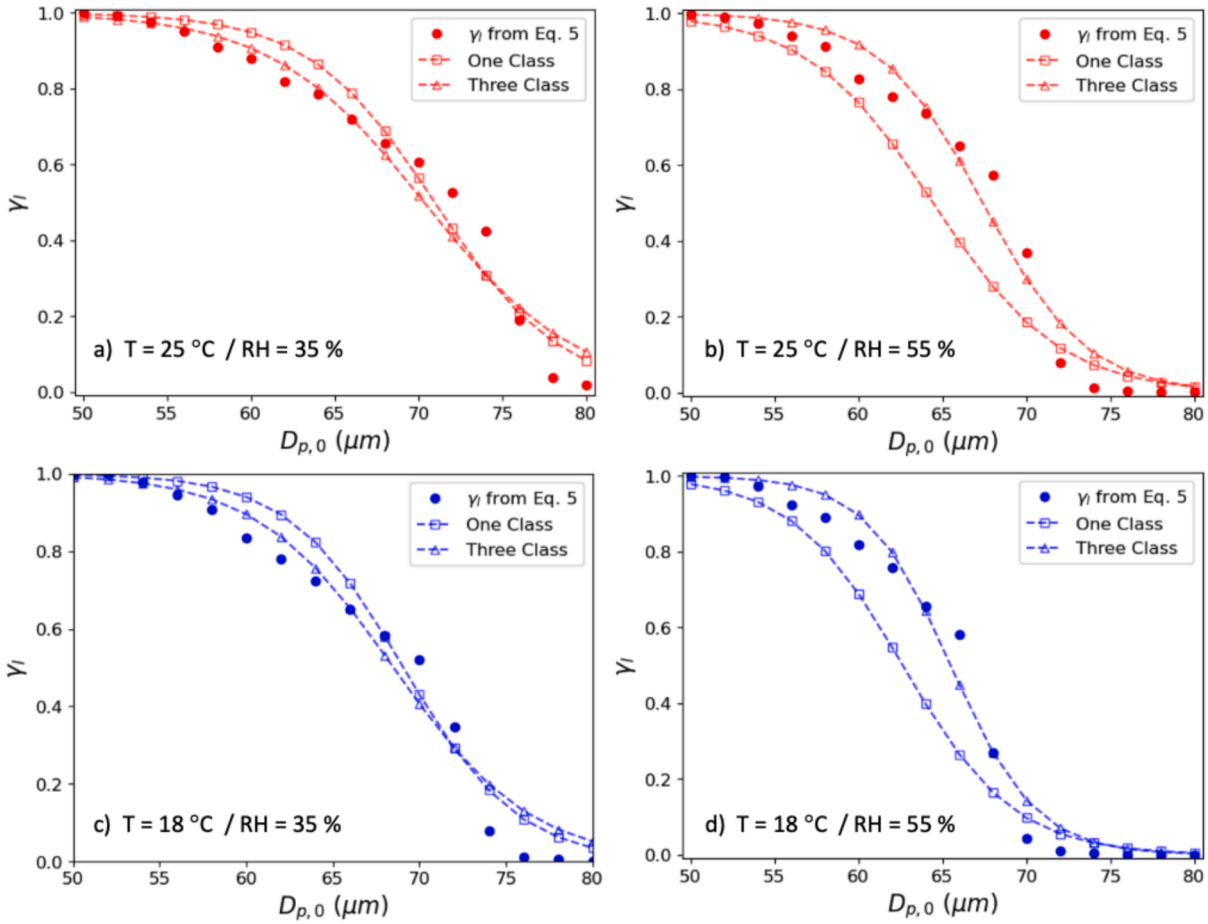


**Fig. 3.** Long-range airborne probability when RH is (a, c) 35 % and (b, d) 55 % for (a, b) summer and (c, d) winter temperatures during coughing simulated using full model from Eq. (5) (circle), One (square) and Three Class (triangle) RH approaches fit to Eq. (6).

**Table 5**
Metrics (Section 2.2.1) used to evaluate cases when the RH is 35 and 55 %, with summer and winter temperatures, using One and Three RH class approaches.

| Model | RH = 35 % | | | RH = 55 % | | |
|---|---|---|---|---|---|---|
| | MAE | MBE | $R^2$ | MAE | MBE | $R^2$ |
| Summer One | 0.055 | −0.023 | 0.959 | 0.092 | 0.070 | 0.894 |
| Summer Three | 0.046 | 0.000 | 0.963 | 0.049 | −0.002 | 0.975 |
| Winter One | 0.058 | −0.039 | 0.963 | 0.087 | 0.067 | 0.907 |
| Winter Three | 0.050 | −0.020 | 0.970 | 0.038 | −0.020 | 0.983 |

## 4. Limitations of this study

In our study, we calculate quanta emission rates without accounting for infectivity decays, ventilation or filtration after exhalation, rather we focus on particles remaining airborne without settling (deposition). However, once IRPs are expelled from the mouth, their infectivity and aerostability are affected by factors such as UV irradiation, ambient $CO_2$ concentration, temperature and relative humidity (Dabisch et al., 2021; Haddrell et al., 2024).

We consider a well-mixed stagnant indoor environment where ventilation does not directly affect the expired jet, yet ventilation designs could play an important role in mitigating airborne transmission risk (Bhagat et al., 2020). Targeted ventilation strategies, such as downward-directed airflows that enhance droplet settling could reduce airborne IRPs by increasing the surface deposition (Pandey et al., 2023). Similarly, prioritizing displacement ventilation over mixing ventilation, where feasible, may help limit fast dilution across the space and minimize the impact of ambient turbulence which could further increase the airborne residence time of droplets (Sodiq et al., 2021; Wei & Li, 2015). In both scenarios, decreasing ambient temperature could further minimise quanta concentrations.

In our study, we define the threshold distance between short and long-range transmission as 2 m for speaking and 4 m for coughing. While there are no absolute values distinguishing these transmission modes, our choice was based on common assumption that close-proximity for speaking falls within 1.5 – 2 m (Li, 2021b), and that the cough jet can remain suspended in the air for longer compared to speaking breaths, reaching up to 4 m (Bourouiba, 2020). Beyond those distances, we assume droplet concentrations become well mixed in the environment, although in real-world conditions droplet distributions are often uneven and unsteady.

Although quanta emission rates are highly sensitive to viral load in droplets, we assume a constant viral load based on viral load of SARS-CoV-2 as in sputum, despite subject characteristics and contamination stage causing variation between $10^1$ to $10^{11}$ RNA copies $mL^{-1}$, being an important source of uncertainty for quanta calculations (Pan et al., 2020). This assumption extends to all droplet sizes despite evidence suggesting that viral load of SARS-CoV-2 varies with droplet size and that finer droplets (< 5 μm) can carry up to 85 % of the total viral load in some cases across various SARS-CoV-2 variants (Coleman et al., 2022; Tan et al., 2023). These findings could significantly influence quanta emission rates calculations, with a comprehensive analysis across a wider range of droplet sizes and pathogens still being necessary. However, by not considering this variability, our findings are generalisable to other pathogens, which may not exhibit the same behaviour.

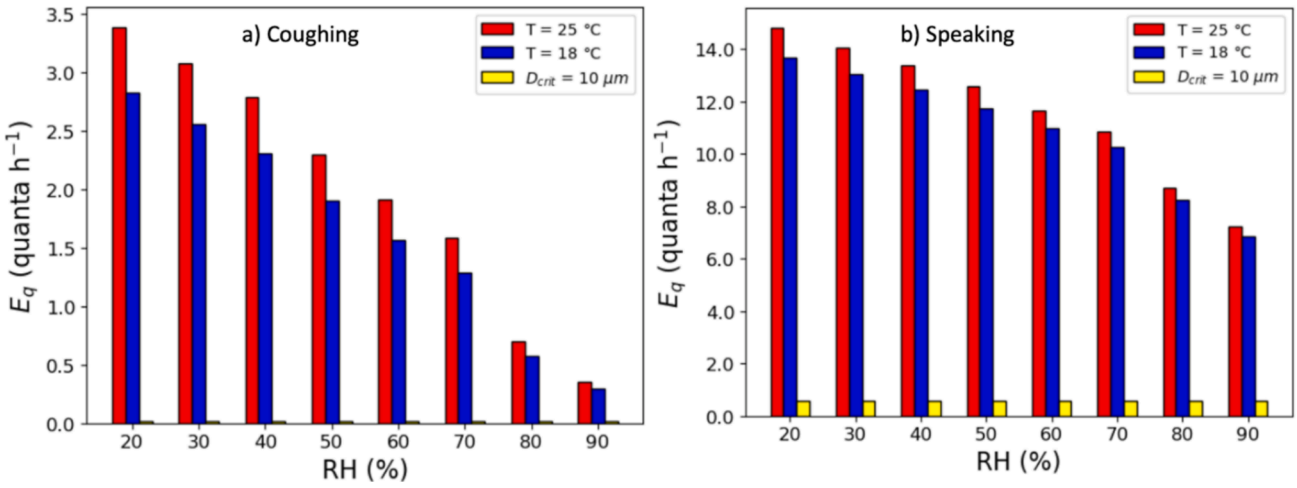


**Fig. 4.** Quanta emission rate for different RH values for summer (red) and winter (blue) temperatures when (a) coughing and (b) speaking when $D_{crit}$ = 100 μm, and if $D_{crit}$ = 10 μm (yellow).

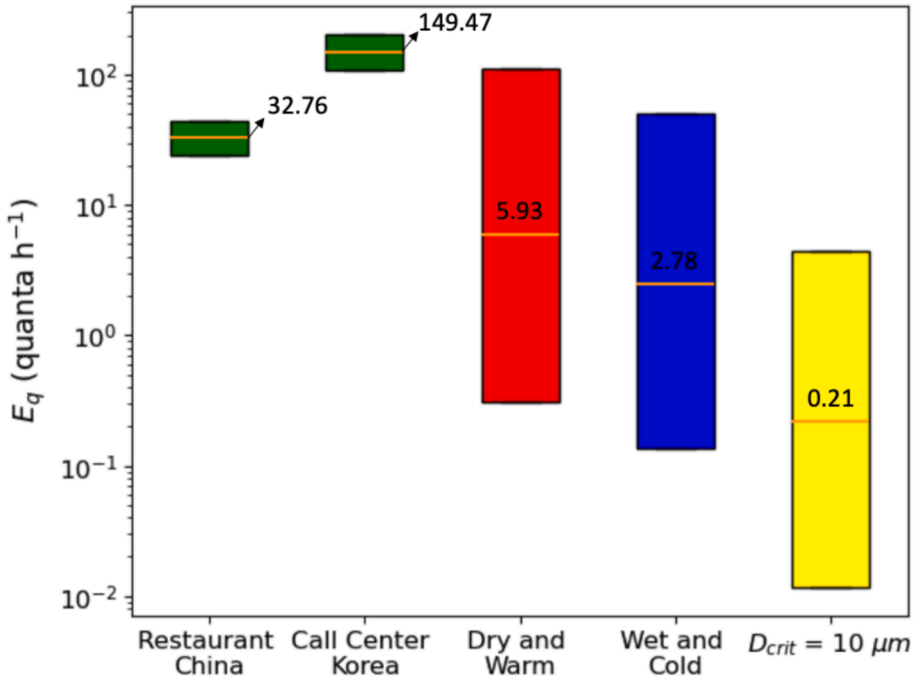


**Fig. 5.** Quanta emission rate for two outbreak cases: a restaurant in China and a call centre in South Korea using the retrospective method (green). Dry and warm (T = 25 °C, RH = 20 %, red) and wet and cold environment (T = 18 °C, RH = 90 %, blue) using our method alongside with the prospective method using $D_{crit}$ = 10 μm. Note Y axis is nonlinear.

## 5. Conclusions

Quantifying the quanta emission rate is crucial for accurate assessment of infectious disease transmission risks. Here we propose a modified prospective method to estimate quanta emission rates that includes both environmental conditions and a larger threshold for inhalable droplet size. Our method employs the long-range airborne probability as a function of indoor relative humidity and temperature, and integrates it together with an exhalation droplet size distribution for coughing and speaking.

Our main findings are that both relative humidity and temperature are important factors in estimating quanta emission rates. Quanta emission rates can be up to 10 times larger in dry indoor environments (RH = 20 %) for coughing and 2 times larger for speaking modes compared to environments with RH = 90 %. Indoor air temperature has a large influence, particularly in dry conditions (RH = 20 %) with winter scenario (T = 18 °C) having a 20 % higher quanta emission rate (cf. summer scenario). These effects are more pronounced for medium-sized droplets (40 – 70 μm), suggesting they could play a crucial role in the inhalation route of disease transmission.

## CRediT authorship contribution statement

**Vitor Lavor:** Writing – original draft, Visualization, Software, Methodology, Formal analysis. **Jianjian Wei:** Methodology, Investigation. **Omduth Coceal:** Writing – review & editing, Supervision. **Sue Grimmond:** Writing – review & editing, Supervision. **Zhiwen Luo:** Writing – review & editing, Supervision, Methodology, Conceptualization.

## Declaration of competing interest

The authors declare that they have no known competing financial interests or personal relationships that could have appeared to influence the work reported in this paper.

## Acknowledgements

VL acknowledges PhD studentship funding from NERC SCENARIO NE/S007261/1.

## Appendix A. Supplementary data

Supplementary data to this article can be found online at https://doi.org/10.1016/j.envint.2025.109379.

## Data availability

Data will be made available on request.

## References

Altshuler, E., Tannir, B., Jolicoeur, G., Rudd, M., Saleem, C., Cherabuddi, K., Doré, D.H., Nagarsheth, P., Brew, J., Small, P.M., Glenn Morris, J., Grandjean Lapierre, S., 2023. Digital cough monitoring – A potential predictive acoustic biomarker of clinical outcomes in hospitalized COVID-19 patients. J. Biomed. Inform. 138, 104283. https://doi.org/10.1016/j.jbi.2023.104283.

Bhagat, R.K., Wykes, M.S.D., Dalziel, S.B., Linden, P.F., 2020. Effects of ventilation on the indoor spread of COVID-19. J. Fluid Mech. 903, F1. https://doi.org/10.1017/jfm.2020.720.

Bourouiba, L., 2020. Turbulent Gas Clouds and Respiratory Pathogen Emissions: Potential Implications for Reducing Transmission of COVID-19. JAMA 323 (18), 1837–1838. https://doi.org/10.1001/jama.2020.4756.

Buonanno, G., Robotto, A., Brizio, E., Morawska, L., Civra, A., Corino, F., Lembo, D., Ficco, G., Stabile, L., 2022. Link between SARS-CoV-2 emissions and airborne concentrations: Closing the gap in understanding. J. Hazard. Mater. 428, 128279. https://doi.org/10.1016/j.jhazmat.2022.128279.

Buonanno, G., Stabile, L., Morawska, L., 2020. Estimation of airborne viral emission: Quanta emission rate of SARS-CoV-2 for infection risk assessment. Environ. Int. 141, 105794. https://doi.org/10.1016/j.envint.2020.105794.

Cavazzuti, M., Tartarini, P., 2023. Transport and evaporation of exhaled respiratory droplets: An analytical model. Phys. Fluids 35 (10), 103327. https://doi.org/10.1063/5.0170545.

Chaudhuri, S., Basu, S., Kabi, P., Unni, V.R., Saha, A., 2020. Modeling the role of respiratory droplets in Covid-19 type pandemics. Phys. Fluids 32 (6), 063309. https://doi.org/10.1063/5.0015984.

Coleman, K.K., Tay, D.J.W., Tan, K.S., Ong, S.W.X., Than, T.S., Koh, M.H., Chin, Y.Q., Nasir, H., Mak, T.M., Chu, J.J.H., Milton, D.K., Chow, V.T.K., Tambyah, P.A., Chen, M., Tham, K.W., 2022. Viral Load of Severe Acute Respiratory Syndrome Coronavirus 2 (SARS-CoV-2) in Respiratory Aerosols Emitted by Patients With Coronavirus Disease 2019 (COVID-19) While Breathing, Talking, and Singing. Clin. Infect. Dis. 74 (10), 1722–1728. https://doi.org/10.1093/cid/ciab691.

Dabisch, P., Schuit, M., Herzog, A., Beck, K., Wood, S., Krause, M., Miller, D., Weaver, W., Freeburger, D., Hooper, I., Green, B., Williams, G., Holland, B., Bohannon, J., Wahl, V., Yolitz, J., Hevey, M., Ratnesar-Shumate, S., 2021. The influence of temperature, humidity, and simulated sunlight on the infectivity of SARS-CoV-2 in aerosols. Aerosol Sci. Tech. 55 (2), 142–153. https://doi.org/10.1080/02786826.2020.1829536.

Duval, D., Palmer, J.C., Tudge, I., Pearce-Smith, N., O'connell, E., Bennett, A., Clark, R., 2022. Long distance airborne transmission of SARS-CoV-2: Rapid systematic review. BMJ 377. https://www.bmj.com/content/377/bmj-2021-068743.long.

Grandoni, L., Pini, A., Pelliccioni, A., Salizzoni, P., Méès, L., Leuzzi, G., Monti, P., 2024. Numerical dispersion modeling of droplets expired by humans while speaking. Air Qual. Atmos. Health. https://doi.org/10.1007/s11869-024-01501-w.

Gupta, J.K., Lin, C.-H., Chen, Q., 2009. Flow dynamics and characterization of a cough. Indoor Air 19 (6), 517–525. https://doi.org/10.1111/j.1600-0668.2009.00619.x.

Haddrell, A., Oswin, H., Otero-Fernandez, M., Robinson, J.F., Cogan, T., Alexander, R., Mann, J.F.S., Hill, D., Finn, A., Davidson, A.D., Reid, J.P., 2024. Ambient carbon dioxide concentration correlates with SARS-CoV-2 aerostability and infection risk. Nat. Commun. 15 (1), 3487. https://doi.org/10.1038/s41467-024-47777-5.

Jimenez, J.L., Marr, L.C., Randall, K., Ewing, E.T., Tufekci, Z., Greenhalgh, T., Tellier, R., Tang, J.W., Li, Y., Morawska, L., Mesiano-Crookston, J., Fisman, D., Hegarty, O., Dancer, S.J., Bluyssen, P.M., Buonanno, G., Loomans, M.G.L.C., Bahnfleth, W.P., Yao, M., Prather, K.A., 2022. What were the historical reasons for the resistance to recognizing airborne transmission during the COVID-19 pandemic? Indoor Air 32 (8), e13070. https://doi.org/10.1111/ina.13070.

Johnson, G.R., Morawska, L., Ristovski, Z.D., Hargreaves, M., Mengersen, K., Chao, C.Y. H., Wan, M.P., Li, Y., Xie, X., Katoshevski, D., Corbett, S., 2011. Modality of human expired aerosol size distributions. J. Aerosol Sci 42 (12), 839–851. https://doi.org/10.1016/j.jaerosci.2011.07.009.

Jones, B., Iddon, C., Sherman, M., 2024. Quantifying quanta: Determining emission rates from clinical data. Indoor Environments 1 (3), 100025. https://doi.org/10.1016/j.indenv.2024.100025.

Jones, B., Iddon, C., Sherman, M.H., 2023. Quantifying Quanta: Why We Can't Be Certain about the Risks of Long-Range Airborne Infection (SSRN Scholarly Paper No. 4595141). https://doi.org/10.2139/ssrn.4595141.

Kroese, D.P., Brereton, T., Taimre, T., Botev, Z.I., 2014. Why the Monte Carlo method is so important today. WIREs Comput. Stat. 6 (6), 386–392. https://doi.org/10.1002/wics.1314.

Kurnitski, J., Kiil, M., Wargocki, P., Boerstra, A., Seppänen, O., Olesen, B., Morawska, L., 2021. Respiratory infection risk-based ventilation design method. Build. Environ. 206, 108387. https://doi.org/10.1016/j.buildenv.2021.108387.

Leung, N.H.L., Milton, D.K., 2024. New WHO proposed terminology for respiratory pathogen transmission. Nat. Rev. Microbiol. 22 (8), 453–454. https://doi.org/10.1038/s41579-024-01067-5.

Li, J., Cheng, Z., Zhang, Y., Mao, N., Guo, S., Wang, Q., Zhao, L., Long, E., 2021. Evaluation of infection risk for SARS-CoV-2 transmission on university campuses. Sci. Technol. Built Environ. 27 (9), 1165–1180. https://doi.org/10.1080/23744731.2021.1948762.

Li, Y., 2021a. Basic routes of transmission of respiratory pathogens—A new proposal for transmission categorization based on respiratory spray, inhalation, and touch. Indoor Air 31 (1), 3–6. https://doi.org/10.1111/ina.12786.

Li, Y., 2021b. Hypothesis: SARS-CoV-2 transmission is predominated by the short-range airborne route and exacerbated by poor ventilation. Indoor Air 31 (4), 921.

Li, Y., Cheng, P., Jia, W., 2022. Poor ventilation worsens short-range airborne transmission of respiratory infection. Indoor Air 32 (1). https://doi.org/10.1111/ina.12946.

Liu, L., Wei, J., Li, Y., Ooi, A., 2017. Evaporation and dispersion of respiratory droplets from coughing. Indoor Air 27 (1), 179–190. https://doi.org/10.1111/ina.12297.

Lu, J., Gu, J., Li, K., Xu, C., Su, W., Lai, Z., Zhou, D., Yu, C., Xu, B., & Yang, Z. (2020). COVID-19 Outbreak Associated with Air Conditioning in Restaurant, Guangzhou, China, 2020—Volume 26, Number 7—July 2020—Emerging Infectious Diseases journal—CDC. 26(7). DOI: 10.3201/eid2607.200764.

Marr, L.C., Tang, J.W., 2021. A Paradigm Shift to Align Transmission Routes With Mechanisms. Clin. Infect. Dis. 73 (10), 1747–1749. https://doi.org/10.1093/cid/ciab722.

Mikszewski, A., Stabile, L., Buonanno, G., Morawska, L., 2022. The airborne contagiousness of respiratory viruses: A comparative analysis and implications for mitigation. Geosci. Front. 13 (6), 101285. https://doi.org/10.1016/j.gsf.2021.101285.

Miller, S.L., Nazaroff, W.W., Jimenez, J.L., Boerstra, A., Buonanno, G., Dancer, S.J., Kurnitski, J., Marr, L.C., Morawska, L., Noakes, C., 2021. Transmission of SARS-CoV-2 by inhalation of respiratory aerosol in the Skagit Valley Chorale superspreading event. Indoor Air 31 (2), 314–323. https://doi.org/10.1111/ina.12751.

Milton, D.K., 2020. A Rosetta Stone for Understanding Infectious Drops and Aerosols. Journal of the Pediatric Infectious Diseases Society 9 (4), 413–415. https://doi.org/10.1093/jpids/piaa079.

Pan, Y., Zhang, D., Yang, P., Poon, L.L.M., Wang, Q., 2020. Viral load of SARS-CoV-2 in clinical samples. Lancet Infect. Dis. 20 (4), 411–412. https://doi.org/10.1016/S1473-3099(20)30113-4.

Pandey, B., Saha, S.K., Banerjee, R., 2023. Effect of ceiling fan in mitigating exposure to airborne pathogens and COVID-19. Indoor Built Environ. 32 (10), 1973–1999. https://doi.org/10.1177/1420326X231154011.

Prentiss, M., Chu, A., Berggren, K.K., 2020. Superspreading events without superspreaders: using high attack rate events to estimate n0 for airborne transmission of COVID-19. medRxiv. https://doi.org/10.1101/2020.10.21.20216895.

Salthammer, T., Morrison, G.C., 2022. Temperature and indoor environments. Indoor Air 32 (5), e13022. https://doi.org/10.1111/ina.13022.

Sodiq, A., Khan, M.A., Naas, M., Amhamed, A., 2021. Addressing COVID-19 contagion through the HVAC systems by reviewing indoor airborne nature of infectious microbes: Will an innovative air recirculation concept provide a practical solution? Environ. Res. 199, 111329. https://doi.org/10.1016/j.envres.2021.111329.

Stadnytskyi, V., Bax, C.E., Bax, A., Anfinrud, P., 2020. The airborne lifetime of small speech droplets and their potential importance in SARS-CoV-2 transmission. Proc. Natl. Acad. Sci. 117 (22), 11875–11877. https://doi.org/10.1073/pnas.2006874117.

Tan, K.S., Ong, S.W.X., Koh, M.H., Tay, D.J.W., Aw, D.Z.H., Nah, Y.W., Abdullah, M.R.B., Coleman, K.K., Milton, D.K., Chu, J.J.H., Chow, V.T.K., Tambyah, P.A., Tham, K.W., 2023. SARS-CoV-2 Omicron variant shedding during respiratory activities. Int. J. Infect. Dis. 131, 19–25. https://doi.org/10.1016/j.ijid.2023.03.029.

Wei, J., Li, Y., 2015. Enhanced spread of expiratory droplets by turbulence in a cough jet. Build. Environ. 93, 86–96. https://doi.org/10.1016/j.buildenv.2015.06.018.

Xie, X., Li, Y., Chwang, A.T.Y., Ho, P.L., Seto, W.H., 2007. How far droplets can move in indoor environments ? Revisiting the Wells evaporation?falling curve. Indoor Air 17 (3), 211–225. https://doi.org/10.1111/j.1600-0668.2007.00469.x.